Time Delay Investigation in Telerobotic Surgery

Vivian Chai and Dan-Sorin Necsulescu
Department of Mechanical Engineering, University of Ottawa, Ottawa, ON, Canada

Keywords: Contact Forces, Robotic Arm Manipulator, Soft Tissue Modelling, Telerobotics, Time Delay.

Abstract: Telerobotic surgery is a medical technology that allows a surgeon to operate on a patient from a distance, via a communication network. As with all telerobotic procedures, factors such as time delay or limited bandwidth may affect the performance of the robotics. In addition, surgeries require contact with soft tissues of the body, resulting in unaccounted external forces on the robotic manipulator. The paper investigates the effects of time delay on the desired trajectory of a telerobotic arm that undergoes forces due to contact with skin tissue. Two behaviours will be explored through simulation, under different time delays, with the robotic arm's end effector sliding across the surface of the skin, as well as compressing the skin perpendicularly. Simulation results are compared with the expected behaviour of existing telerobotic performance. It was found that tangential forces across the skin's surface do not significantly impact telerobotic performance but when subject to normal contact, the robotic arm fails under shorter time delays than expected. Further experimentation with trajectories, not limited to parallel or perpendicular motion of the effector on the skin, and trials involving real tissues and manipulators will provide greater insight for understanding telerobotic performance in surgery.

1 INTRODUCTION

With the improvements of modern technology, telerobotic applications are becoming more prominent in the medical field. These procedures are carried out through a communication network between a user-controlled master console and a semi-autonomous, slave robot that moves based on directions from the user (Avgousti et al., 2016). This networking enables medical treatment to be performed without direct contact between patient and doctor. As telerobotic applications, in the medical field, are still a relatively new subject of research, there are many areas that require progress, which may offer various improvements to the existing health care systems.

Telerobotic surgery, in particular, is a topic of great interest, as it presents many advantages over current surgical procedures. When compared with traditional surgical methods, surgical robots have a significantly greater range of motion and can be smaller than a human hand, allowing for more complex and dexterous movements (Ho et al., 2011). These robots can be small and equipped with various sensors and cameras, resulting in less invasive operations, fewer surgical complications and blood loss, as well as significant reductions in patient recovery time (Buia et al., 2015). Furthermore, with telerobotics, treatment of infectious diseases or surgeries in remote locations can be performed (Arata et al., 2007). These advantages, and many more, encourage the technological advancements of robotics in this field.

However, telerobotic surgeries still have many issues that have yet to be resolved. As these surgeries are highly dependent on the communication feedback from the slave controller, any feedback problems will greatly influence the robot's performance. In particular, time delay during the transmission of information to and from the slave robot is always prevalent in telerobotic operations. These delays prevent up-to-date knowledge from reaching the operator, which may in turn impact performance, depending on the length of the delay. For surgeries, which are time sensitive, these delays are dangerous and can pose a threat to the patient's well being.

This paper explores the effects of time delay on a 3-linkage planar robotic arm, operating in a surgical environment. Different interactions, such as tangeantial surface contact and compression between the soft tissue and robotic arm, will be modeled and simulated under different time delays, and performance of the robot will be compared to its desired movement. Simulations were performed using MATLAB™and Simulink™.

Chai, V. and Necsulescu, D.
Time Delay Investigation in Telerobotic Surgery.
DOI: 10.5220/0010515603750382
In *Proceedings of the 18th International Conference on Informatics in Control, Automation and Robotics (ICINCO 2021)*, pages 375-382
ISBN: 978-989-758-522-7

2 BACKGROUND

The concepts of time delay, manipulator control, and soft tissue behaviour in the surgical environment must be understood. The following section presents the knowledge about these topics that is required for modeling.

2.1 Time Delay

All telerobotic operations have time delays, which stem from a combination of delays from image capturing, communications, signal processing for the controllers and many more factors (Vazquez-Santacruz et al., 2017)(Velasco-Villa et al., 2013). Many studies have shown that as time delay increases, the number of moves required, the time to complete the task, as well as the number of errors all increase (Fabrizio et al.,)(Anvari et al., 2005)(Lum et al., 2009)(Korte et al., 2014)(Hristu et al., 1996)(M. Uebel et al., 1994). However, it is important to note that while time delays cannot be completely eliminated from a system, shorter time delays are beneficial to the system's performance. Table 1 below shows the effects of different time delays on their performance, gathered from various papers (Orosco et al., 2020)(Perez et al., 2015)(Xu et al., 2014).

Table 1: Time Delay Effects on Telerobotic Performance.

Delay Length (ms)	Telerobotic Performance
No Time Delay	No Effect.
0−300	Task duration increased. No performance effects.
300−500	Task duration increased. Increase in errors.
500−700	Possible task failure. Increase in errors.
700+	Error in every task.

For tasks with time delays between 500ms - 700ms, performance is heavily dependent on the operator's experience. More experienced operators may have fewer errors and succeed in tasks that inexperienced ones would fail (Ladoiye et al., 2018).

2.2 Manipulator Control

2.2.1 Model Predictive Control

Model Predictive Controllers (MPCs) are effective controllers that use an iterative prediction and optimization process to generate ideal outputs. This is done by combining actual values, obtained from the slave manipulator, with predicted values from the master controller, and reference values from the input, to create variety of possible control signal outputs over a specified prediction horizon (Camacho and Bordons, 2007)(Wang, 2009). From these outputs, the best trajectory is selected based on a cost function, and a single time step from the prediction is applied to the system. The process is then repeated for the next time step. Figure 1 below shows the MPC prediction process for a given prediction horizon of p.

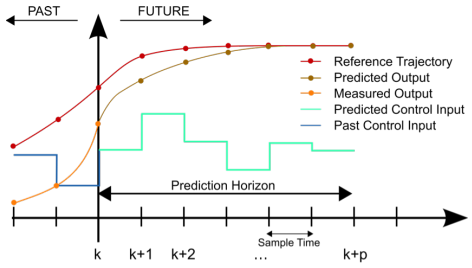

Figure 1: Model Predictive Control Output Prediction Process (Simon, 2014).

An advantage of MPCs is its compatibility with multiple input and multiple output (MIMO) systems. This is useful for robotic arm applications, as torques from the torque from the joints affect one another.

2.2.2 System Dynamics

The motion of a manipulator can be described by its equations of motion, which define a relationship between the input torques and the output manipulator movement (Spong et al., 2005). The general matrix formulation of the equations of motion are shown in Equation (1) below.

$$M(q)\ddot{q} + V(q,\dot{q})\dot{q} + g(q) = \tau \tag{1}$$

where $D(q)$, $V(q,\dot{(q)})$, and $g(q)$ represent the mass matrix, the joint velocity terms, and the gravity vector respectively. The joint velocity matrix can be split into two terms: the centrifugal, $C(q)$ and coriolis, $B(q)$ forces.

A method of obtaining the system dynamics is via the Lagrangian formulation, which is derives equations using the energies of the system (Asada and Slotine, 1986). Equation (2) is the Euler-Lagrange that must be computed to obtain the equations of motion, while Equation (3) provides the Lagrangian, which is the difference between kinetic and potential energies.

$$\frac{d}{dt}\frac{\partial \mathcal{L}}{\partial \dot{q}_i} - \frac{\partial \mathcal{L}}{\partial q_i} = \tau \tag{2}$$

$$\mathcal{L} = K - V \tag{3}$$

Implementing the computed energies into Equation

(2) and Equation (3) will give the system dynamics in the form of Equation (1).

2.3 Soft Tissue Modeling

2.3.1 Soft Tissue Behaviour

To model and simulate interactions between the robot and soft tissue, the soft tissue properties must be fully understood. Tissues exhibit hyperelastic and viscoelastic behaviour and factors such as its composition affect how the material reacts to contact. These combined characteristics make it very difficult to accurately model soft tissues

The hyperelastic behaviour of the tissue indicates that deformations do not occur linearly with applied force. A study, summarized in (Misra et al., 2008), showed that the stress-strain relationship is linear, only if deformations are within 1-2% of the tissues original shape. Successful models, such as the Ogden, Yeoh, and Arruda-Boyce models, which accurately represent this hyperelastic behaviour, have been developed (Bergström, 2015). Figure 2 below shows a general stress-strain curve for the behaviour of hyperelastic materials, where the curved line represents the line of best fit for experimental results.

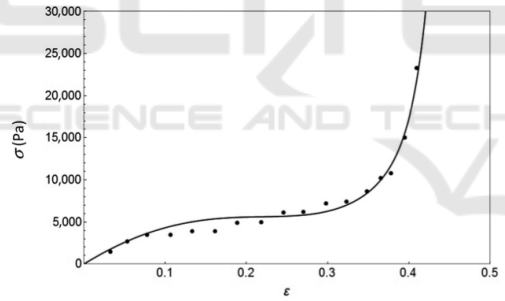

Figure 2: General Stress-Strain Relationship of a Hyperelastic Material (Amabili, 2018).

Soft tissues, with their viscoelastic properties, will have both 'elastic' and 'viscous' behaviour. The 'elastic' term indicates that the tissues will return back to their original form after deformation, and the 'viscous' term indicates that stress on the tissue increases with strain, meaning that the material becomes more resistant to deformation the more it is compressed/stretched (Gould et al., 2019). When modeling these characteristics, the elastic and viscous behaviours can be modeled by springs and dampers respectively.

Another factor to consider when modeling tissues is the effect of its composition. Different tissue types, such as epithelial, muscle, etc., will have different properties. In addition, tissues are made of different quantities of cells, elastin, collagen, and other components, set in different arrangements and at different orientation (Famaey and Sloten, 2008). These quantities, arrangements, and orientations can change how the material reacts to various forces applied to it. The composition of the tissues, which differs from patient to patient, make accurate modeling very difficult.

2.3.2 Hunt-Crossley Method

An established non-linear model, called the Hunt-Crossley method, is able to capture both hyperelastic and viscoelastic behaviour of soft tissues (Pappalardo et al., 2016). This model is shown below, in Figure 3, and its corresponding equation is described by (4).

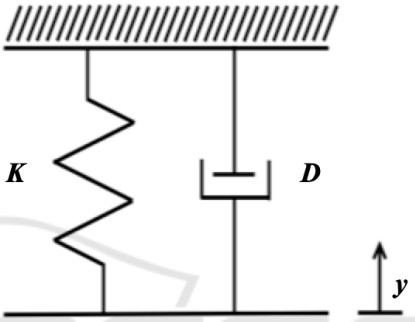

Figure 3: Hunt-Crossley Soft Tissue Model (Amabili, 2018).

$$F = ky^{\beta}(t) + \lambda y^{\beta}(t)\dot{y}(t) \tag{4}$$

where parameters k, β, and λ are obtained experimentally. Thus, from Figure 3 and (4), variables K and D are defined as $K = ky^{\beta-1}(t)$ and $D = \lambda y^{\beta}(t)$ respectively. The exponential factor, β, illustrates the non-linear stress-strain tissue relationship, due to hyperelasticity, while the first and second terms show the elastic and viscous characteristics of the tissue respectively (Pappalardo et al., 2016). The Hunt-Crossley method is currently one of the most accurate soft tissue models that can be solved without the use of complex operations such as continuum-mechanics and finite element analysis.

3 SYSTEM SETUP

The block diagram from Figure 4 shows the general setup of a telerobotic system in a surgical setting. It consists of an operating the master console, a slave console, and a communication network that connects the two. Note that the network can experience time delay and/or discontinuity when transferring information between the two locations.

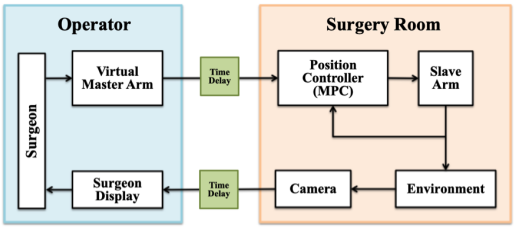

Figure 4: Block Diagram Showing a Telerobotic Surgery Setting.

For simulations, two main components must be modeled for the setup: the slave robot manipulator and the surrounding environment, the soft tissue. The simulation focuses on the slave manipulator with transport delays used to model the telerobotic aspect of the system. Models for these parts are described below.

3.1 Robot Manipulator

The robotic arm used in this paper is a planar 3DOF RRR robot, as shown below in Figure 5. An MPC will be used to control that arm. All linkages are the same length and its properties are shown in Table 2 (Atlas Steels Technical Department, 2013).

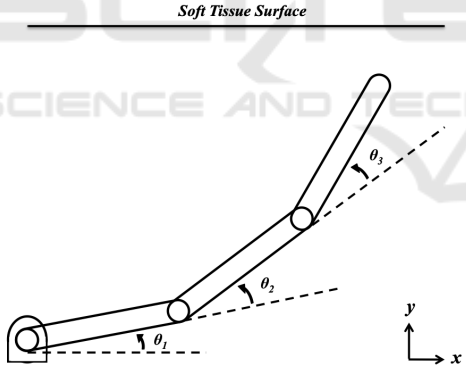

Figure 5: 3DOF Robotic Arm and Surface Diagram.

Table 2: 3DOF Robotic Arm Diagram.

Property	Magnitude
Length (cm)	10
Radius (cm)	1
Density (g/cm^2)	7.95

Robotic arms used for surgical purposes are usually very small, as shown by the small dimensions in the table above. While these dimensions do not come from any existing robotic arm, they are selected to give a size similar to the da Vinci SP surgical robot (Cruz et al., 2019).

The equations of motion for the arm, derived using the Lagrangian Formulation, are presented in Equation (5).

$$\begin{bmatrix} A_1 & B_1 & C_1 \\ D_1 & E_1 & F_1 \\ G_1 & H_1 & I_1 \end{bmatrix} \begin{bmatrix} \ddot{\theta}_1 \\ \ddot{\theta}_2 \\ \ddot{\theta}_3 \end{bmatrix} + \begin{bmatrix} A_2 & B_2 & C_2 \\ D_2 & E_2 & F_2 \\ G_2 & H_2 & I_2 \end{bmatrix} \begin{bmatrix} \dot{\theta}_1^2 \\ \dot{\theta}_2^2 \\ \dot{\theta}_3^2 \end{bmatrix} + \begin{bmatrix} A_3 & B_3 & C_3 \\ D_3 & E_3 & F_3 \\ G_3 & H_3 & I_3 \end{bmatrix} \begin{bmatrix} \dot{\theta}_1\dot{\theta}_2 \\ \dot{\theta}_1\dot{\theta}_3 \\ \dot{\theta}_2\dot{\theta}_3 \end{bmatrix} = \begin{bmatrix} \tau_1 \\ \tau_2 \\ \tau_3 \end{bmatrix} \quad (5)$$

where

$A_1 = 0.5ml^2[(c_{1+12} - s_{1+12})^2 + (c_{1+12+123} - s_{1+12+123})^2] + ms_1^2$

$B_1 = D_1 = 0.5ml^2[(c_{12} - s_{12})(c_{1+12} - s_{1+12}) - (c_{12+123} - s_{12+123})(c_{1+12+123} - s_{1+12+123})] - ms_1s_2$

$C_1 = G_1 = 0.5ml^2(c_{123} - s_{123})(c_{1+12+123} - s_{1+12+123})$

$E_1 = 0.5ml^2[(c_{12+123} - s_{12+123})^2 + (c_{12} - s_{12})^2] + ms_2^2$

$F_1 = H_1 = 0.5ml^2(c_{123} - s_{123})(c_{12+123} - s_{12+123})$

$I_1 = 0.5ml^2(c_{123} - s_{123})^2$

$A_2 = 0.5ml^2[(c_{1+12+123} - s_{1+12+123})(c_{1+12+123} + s_{1+12+123}) + (c_{1+12} + s_{1+12})(c_{1+12} - s_{1+12})] - mc_1s_1$

$B_2 = 0.5ml^2[(c_{12+123} + s_{12+123})(c_{12+123} - s_{12+123}) + (c_{12} - s_{12})(c_{12} + s_{12})]$

$C_2 = 0.5ml^2(c_{123} - s_{123})(c_{123} + s_{123})$

$D_2 = 0.5ml^2[(c_{12} + s_{12})(c_{1+12} - s_{1+12}) + (c_{12+123} + s_{12+123})(c_{1+12+123} - s_{1+12+123})]$

$E_2 = 0.5ml^2[(c_{12+123} + s_{12+123})(c_{12+123} - s_{12+123}) + (c_{12} - s_{12})(c_{12} + s_{12})] - mc_2s_2$

$F_2 = 0.5ml^2(c_{123} - s_{123})(c_{123} + s_{123})$

$G_2 = 0.5ml^2(c_{123} + s_{123})(c_{1+12+123} - s_{1+12+123})$

$H_2 = 0.5ml^2(c_{123} + s_{123})(c_{12+123} - s_{12+123})$

$I_2 = 0.5ml^2(c_{123} - s_{123})(c_{123} + s_{123})$

$A_3 = 0.5ml^2[(c_{12} + s_{12})(c_{1+12} - s_{1+12}) + (c_{12+123} - s_{12+123})(c_{1+12+123} + s_{1+12+123}) + (c_{12} - s_{12})(c_{1+12} + s_{1+12}) + (c_{12+123} + s_{12+123})(c_{1+12+123} - s_{1+12+123})] - mc_1s_2$

$B_3 = 0.5ml^2[(c_{123} - s_{123})(c_{1+12+123} + s_{1+12+123}) + (c_{123} + s_{123})(c_{1+12+123} - s_{1+12+123})]$

$C_3 = 0.5ml^2[(c_{123} + s_{123})(c_{12+123} - s_{12+123}) + (c_{123} - s_{123})(c_{12+123} + s_{12+123})]$

$D_3 = 0.5ml^2[(c_{12} + s_{12})(c_{1+12} - s_{1+12}) + (c_{12+123} + s_{12+123})(c_{1+12+123} - s_{1+12+123}) + (c_{12+123} + s_{12+123})(c_{12+123} - s_{12+123}) + (c_{12} - s_{12})(c_{12} + s_{12})] - mc_2s_1$

$E_3 = 0.5ml^2[(c_{123} - s_{123})(c_{12+123} + s_{12+123}) + (c_{123} + s_{123})(c_{1+12+123} - s_{1+12+123})]$

$F_3 = 0.5ml^2[(c_{123} + s_{123})(c_{12+123} - s_{12+123}) + (c_{123} - s_{123})(c_{12+123} + s_{12+123})]$

$G_3 = 0.5ml^2[(c_{123} + s_{123})(c_{12+123} - s_{12+123}) + (c_{123} + s_{123})(c_{1+12+123} - s_{1+12+123})]$

$H_3 = 0.5ml^2[(c_{123} + s_{123})(c_{1+12+123} - s_{1+12+123}) + (c_{123} - s_{123})(c_{123} + s_{123})]$

$I_3 = 0.5ml^2[(c_{123} + s_{123})(c_{12+123} - s_{12+123}) + (c_{123} - s_{123})(c_{123} + s_{123})]$

Note that c_{ab} represents $cos(a+b)$ while c_{a+b} represents $cos(a)+cos(b)$. All s terms represent the *sine* counterparts. There is also no gravity term because the gravitational force acts in the axis of the joint rotation, therefore it does not significantly affect the motion of the arm.

3.2 Soft Tissue

The Hunt-Crossley method will be used to model the soft tissue, as this method is able to capture various characteristics of the tissue, while maintaining model simplicity. The parameters below, provided in Table 3 and Table 4 will be used. Table 3 shows the parameters for perpendicular contact forces between the soft tissue and a metal part, while Table 4 provides corresponding properties for skin tissue (Liang and Bopart, 2010)(Veijgen, 2013). The selected parameters for the normal force are average values obtained from five experimental trials of a robot interacting with soft tissue reported in (Yamamoto et al., 2009).

Table 3: Experimental Hunt-Crossley Parameters.

k	5.5432
λ	0.1496
β	1.5826

Table 4: Soft Tissue Behavioural Parameters.

Parameters	Value
Coefficient of Static Friction	0.52
Coefficient of Kinetic Friction	0.36
Skin Density (kg/m^3)	1.02

4 RESULTS

Two scenarios will be simulated for the robot and soft tissue interaction under different time delays. The first simulation involves a robotic arm moving to approach a soft tissue surface, where it will then slide tangentially across the surface of the skin. For the second scenario, the robotic arm will come in contact with the tissue surface, where it will then attempt to compress the tissue. Figure 6 below shows the intended trajectories for both simulations.

The input trajectory, from Figure 6 is converted from Cartesian coordinates to joint coordinates, via inverse kinematics, and is then converted into joint torques using the controller.

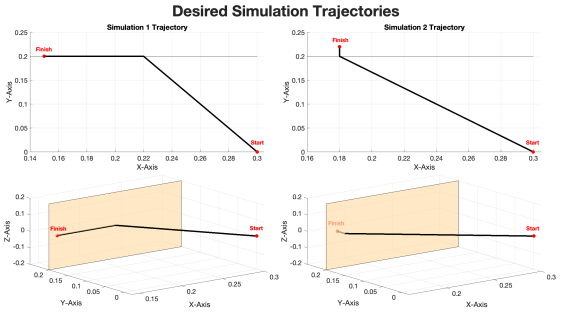

Figure 6: Desired Trajectory of the Robotic Arm for Both Simulations.

4.1 Scenario 1: Movement across the Tissue

In scenario 1, the path of the robotic arm's end effector will be traced, namely the movement across the skin, in the Y-direction, and the frictional and normal forces will be recorded. The tissue sample is located 0.2m away from the robot's starting position and the surface should be reached, in the simulation, in 7 seconds. Results of the simulations are shown below and will be compared to the expected performance results presented in Table 1.

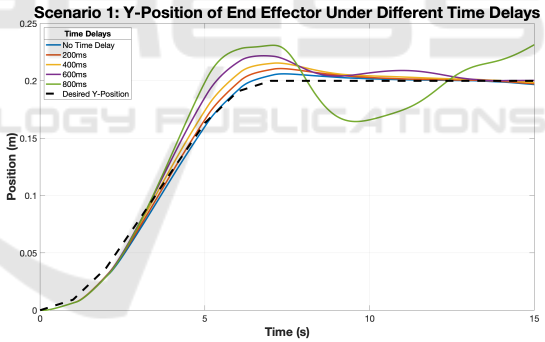

Figure 7: End Effector Position in the Y-Direction.

From Figure 7, it can be seen that all simulations, with the exception of the 800ms time delay trial, reach the desired final position of 0.2m. It is noted, however, that with increased time delay, the magnitude of the errors also increases, and the system requires more time to reach its desired value. In addition, although the simulation trajectory is planned to have no contact with the soft tissue, all scenarios are shown to have slight interactions, which result in forces on the tissue and robot. This behaviour can be seen in more detail in Figure 8 and Figure 9, which show the contact and frictional forces computed during simulation. The simulation for a time delay 800ms is not included in friction results as the task has already failed.

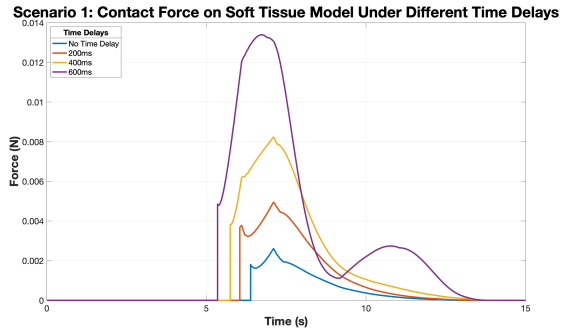

Figure 8: Contact Force between the End Effector and Soft Tissue along the Y-Direction.

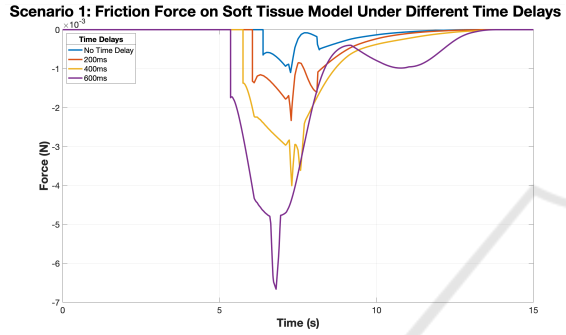

Figure 9: Frictional Force between the End Effector and Soft Tissue along the X-Direction.

Note that the normal force and frictional force points correspond with one another, as both will occur once the robot is in contact with tissue. These points also correspond to points from Figure 7, where the end effector position peaks and is recorded to be above 0.2m. Greater contact and frictional forces also occur for longer time delays. It is interesting to note that although the planned trajectory is to move the robot across the surface of the tissue, the normal contact forces are stronger than the frictional forces.

Upon immediate contact with the skin, at 7 seconds, the robotic arm briefly moves slightly away from its position, before continuing to penetrate the skin surface. Figure 8 shows the reduction in contact force due to this movement. This behaviour is likely due to the interaction with the soft tissue. As previously explained, soft tissue exhibits a viscoelastic property, which would result in the end effector being repelled from the surface of the skin. This results in unstable contact.

The observations from this simulation match with the expected behaviour of telerobotics under time delay, as presented in Table 1. Increasing time delay increases the system errors and the time required to complete the desired task. In addition, the simulated trial with a time delay of over 700ms failed, as expected.

4.2 Scenario 2: Movement into the Tissue

In this scenario, the tissue sample is located 0.2m away from the skin surface, and the robot attempts to penetrate the skin by 2cm, for a total desired displacement of 0.22m. Initial contact with the skin occurs at 6 seconds, and the robot arm is held in place, at a desired compression of 0.22m, after 13 seconds. Interesting properties to observe include the path of the robot, as it attempts to compress the skin tissue, as well as the total penetration into the tissue and the corresponding contact forces. Figure 10 below shows the movement of the tip of the robot compared to the desired movement.

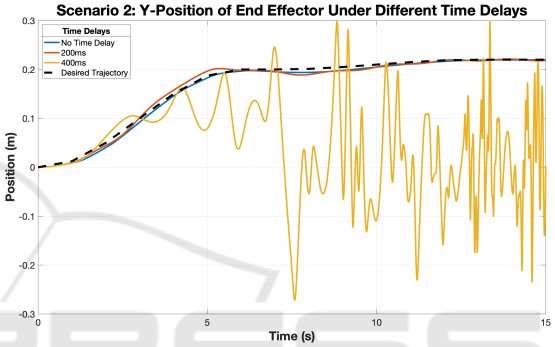

Figure 10: End Effector Position in the Y-Direction.

For this scenario, only time delay simulations of up to 400ms are included, as the erratic movement of the arm indicates system failure. Given that the purpose of these robots is for surgery, an uncontrolled and large displacement is very dangerous and unsuitable for the application.

Figure 11 shows the penetration distance of the soft tissue. The simulated 400ms time delay is not included in these results, due to failure. Again, the trial with no time delay approaches the desired state much faster than the trial with a 200ms delay. Furthermore, the penetration error is larger for the 200ms delay trial, with more oscillations, indicating greater instability in the system. Errors are expected to be even larger for larger delays.

Figure 12 shows the normal contact forces, which correspond to the penetration distances above. Recall that the contact force is proportional to the penetration distance, but the relationship is non-linear, as described by the Hunt-Crossley model in Equation 4.

When compared with Scenario 1, where contact and penetration were not intended, the contact forces due to compression are significantly larger. Frictional forces were neglected for this scenario, as they are expected to be very small, since motion is penetrative.

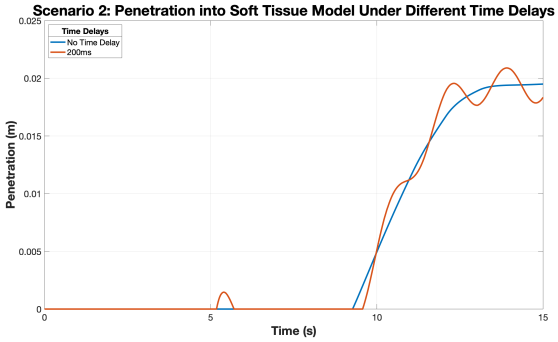

Figure 11: Penetration Depth of the End Effector into the Soft Tissue.

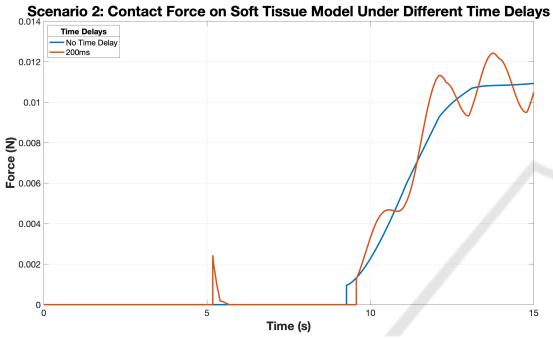

Figure 12: Contact Force between the End Effector and Soft Tissue.

It should be noted that the rebounding behaviour upon initial contact, mentioned in Scenario 1, can clearly be seen in both Figure 11 and Figure 12. The change in motion and force, shown for the simulation with a time delay of 200ms, indicates instability from contact with the body.

In general, the performance of the robot during compression of soft tissue, is similar to the behaviour described by Table 1. As time delay increases, the errors increase, and the desired position is achieved at a much slower rate. However, in this scenario the system fails at a delay of 400ms, instead of the 700ms+ time delay expected from the performance information in Table 1. It is likely that this occurred because the system was unable to adapt to the force from the contact with the tissue in combination with the delayed feedback response. The time delay increases the position error, resulting in greater compression and a larger rebounding force, resulting in uncontrolled displacement of the arm. Thus, under these conditions, the desired task cannot be completed with a time delay of 400ms.

5 CONCLUSION

This paper and the performed simulations are designed to help get a better understanding of the behaviour of telerobotic contact with soft tissues. Under small time delays, it appears that the 3DOF RRR robotic arm is able to carry out desired tasks in a surgical environment. However, large time delays, as well as large forces from contact with the tissues result in task failure. The motion, due to the these forces, is difficult to predict, and the system is unable to compensate for large, unpredicted forces.

In addition, the direction in which the robot comes in contact with the surface also influences the success of a task. The forces generated by perpendicular contact with a surface are significantly larger than those that are tangential and as a result they destabilize the system more and have a greater effect on robot performance. Simulating trials with different trajectories, which have both significant frictional and normal contact forces, and examining the force effects may be considered for future work. Experimentation with real tissue and telerobotic manipulators would also be beneficial for further investigation.

REFERENCES

Amabili, M. (2018). *Hyperelasticity of Soft Biological and Rubber Materials*, page 151–224. Cambridge University Press.

Anvari, M., Broderick, T., Stein, H., Chapman, T., Ghodoussi, M., Birch, D. W., Mckinley, C., Trudeau, P., Dutta, S., and Goldsmith, C. H. (2005). The Impact of Latency on Surgical Precision and Task Completion during Robotic-Assisted Remote Telepresence Surgery. *Computer Aided Surgery*, 10(2):93–99.

Arata, J., Takahashi, H., Pitakwatchara, P., Warisawa, S., Tanoue, K., Konishi, K., Ieiri, S., Shimizu, S., Nakashima, N., Okamura, K., Fujino, Y., Ueda, Y., Chotiwan, P., Mitsuishi, M., and Hashizume, M. (2007). A Remote Surgery Experiment between Japan and Thailand over Internet using a Low Latency CODEC System. In *Proceedings 2007 IEEE International Conference on Robotics and Automation*, pages 953–959, Rome, Italy. IEEE. ISSN: 1050-4729.

Asada, H. and Slotine, J. (1986). *Robot Analysis and Control*. A Wiley-Interscience Publication. Wiley.

Atlas Steels Technical Department (2013). Stainless Steel Grade Datasheets. *Atlas Technical Handbook of Stainless Steels*.

Avgousti, S., Christoforou, E., Panayides, A., Voskarides, S., Novales, C., Nouaille, L., Pattichis, C., and Vieyres, P. (2016). Medical Telerobotic Systems: Current Status and Future Trends. *BioMedical Engineering Online*, 15.

Bergström, J. (2015). 5 - Elasticity/Hyperelasticity. In Bergström, J., editor, *Mechanics of Solid Polymers*, pages 209 – 307. William Andrew Publishing.

Buia, A., Stockhausen, F., and Hanisch, E. (2015). Laparoscopic Surgery: A Qualified Systematic Review. *World Journal of Methodology*, 5:238–54.

Camacho, E. F. and Bordons, C. (2007). Introduction to Model Predictive Control. In Camacho, E. F. and Bordons, C., editors, *Model Predictive Control*, pages 1–11. Springer London, London.

Cruz, C., Yang, H., Kang, I., Kang, C., and Lee, W. (2019). Technical Feasibility of da Vinci SP Single-Port Robotic Cholecystectomy: A Case Report. *Annals of Surgical Treatment and Research*, 97:217.

Fabrizio, M., Lee, B., Chan, D., Stoianovici, D., Jarrett, T., Yang, C., and Kavoussi, Louis, m. . m. y. . . p. . . Effect of Time Delay on Surgical Performance during Telesurgical Manipulation. *Journal of Endourology / Endourological Society*, 14.

Famaey, N. and Sloten, J. V. (2008). Soft Tissue Modelling for Applications in Virtual Surgery and Surgical Robotics. *Computer Methods in Biomechanics and Biomedical Engineering*, 11(4):351–366.

Gould, T. E., Jesunathadas, M., Nazarenko, S., and Piland, S. G. (2019). Chapter 6 - Mouth Protection in Sports. In Subic, A., editor, *Materials in Sports Equipment (Second Edition)*, pages 199–231. Woodhead Publishing.

Ho, C., Tsakonas, E., Tran, K., Cimon, K., Severn, M., Mierzwinski-Urban, M., Corcos, J., and Pautler, S. (2011). Robot-Assisted Surgery Compared with Open Surgery and Laparoscopic Surgery: Clinical Effectiveness and Economic Analyses.

Hristu, D., Kontarinis, D. A., and Howe, R. D. (1996). A Comparison of Delay and Bandwidth Limitations in Teleoperation. *13th World Congress of IFAC, 1996, San Francisco USA, 30 June - 5 July*, 29(1):5709–5714.

Korte, C., Nair, S., Nistor, V., Low, T., Doarn, C., and Schaffner, G. (2014). Determining the Threshold of Time-Delay for Teleoperation Accuracy and Efficiency in Relation to Telesurgery. *Telemedicine Journal and E-Health : The Official Journal of the American Telemedicine Association*, 20.

Ladoiye, J., Necsulescu, D., and Sasiadek, J. (2018). Force Control of Surgical Robot with Time Delay using Model Predictive Control. pages 202–210.

Liang, X. and Boppart, S. A. (2010). Biomechanical Properties of In Vivo Human Skin from Dynamic Optical Coherence Elastography. *IEEE Transactions on Bio-Medical Engineering*, 57(4):953–959. Edition: 2009/10/09.

Lum, M., Rosen, J., King, H. H., Friedman, D., Lendvay, T., Wright, A., and Hannaford, B. (2009). Teleoperation in Surgical Robotics - Network Latency Effects on Surgical Performance. *Conference Proceedings : Annual International Conference of the IEEE Engineering in Medicine and Biology Society*, 2009:6860–3.

M. Uebel, M. Ali, and I. Minis (1994). The Effect of Bandwidth on Telerobot System Performance. *IEEE Transactions on Systems, Man, and Cybernetics*, 24(2):342–348.

Misra, S., Ramesh, K. T., and Okamura, A. M. (2008). Modeling of Tool-Tissue Interactions for Computer-Based Surgical Simulation: A Literature Review. *Presence: Teleoperators and Virtual Environments*, 17(5):463–491.

Orosco, R., Lurie, B., Matsusaki, T., Funk, E., Divi, V., Holsinger, C., Hong, S., Richter, F., Das, N., and Yip, M. (2020). Compensatory Motion Scaling for Time-Delayed Robotic Surgery. *Surgical Endoscopy*.

Pappalardo, A., Albakri, A., Liu, C., Bascetta, L., De Momi, E., and Poignet, P. (2016). Hunt–Crossley Model based Force Control for Minimally Invasive Robotic Surgery. *Biomedical Signal Processing and Control*, 29:31–43.

Perez, M., Xu, S., Chauhan, S., Tanaka, A., Simpson, K., Abdul-Muhsin, H., and Smith, R. (2015). Impact of Delay on Telesurgical Performance: Study on the Robotic Simulator dV-Trainer. *International Journal of Computer Assisted Radiology and Surgery*, 11.

Simon, D. (2014). *Model Predictive Control in Flight Control Design - Stability and Reference Tracking*. PhD thesis.

Spong, M., Hutchinson, S., and Vidyasagar, M. (2005). *Robot Modeling and Control*. Wiley.

Vazquez-Santacruz, J. A., Velasco-Villa, M., Portillo-Velez, R. d. J., Marin-Urias, L. F., and Vigueras-Zuniga, M. (2017). Autonomous Navigation for Multiple Mobile Robots under Time Delay in Communication. *Journal of Intelligent & Robotic Systems*, 86(3-4):583–597.

Veijgen, N. (2013). *Skin Friction: A Novel Approach to Measuring In Vivo Human Skin*. PhD thesis, University of Twente, Netherlands.

Velasco-Villa, M., Castro-Linares, R., Rosales-Hernández, F., del Muro-Cuéllar, B., and Hernández-Pérez, M. (2013). Discrete-Time Synchronization Strategy for Input Time-Delay Mobile Robots. *Journal of the Franklin Institute*, 350(10):2911–2935.

Wang, L. (2009). Model Predictive Control System Design and Implementation Using MATLAB®. ISSN: 1430-9491.

Xu, S., Perez, M., Yang, K., Perrenot, C., Felblinger, J., and Hubert, J. (2014). Determination of the Latency Effects on Surgical Performance and the Acceptable Latency Levels in Telesurgery Using the dV-Trainer (R) simulator. *Surgical Endoscopy*, 28.

Yamamoto, T., Vágvölgyi, B., Balaji, K., Whitcomb, L., and Okamura, A. (2009). Tissue Property Estimation and Graphical Display for Teleoperated Robot-Assisted Surgery. *2009 IEEE International Conference on Robotics and Automation*, pages 4239–4245.